Int. J. Electrochem. Sci., 9 **(2014)** 1187 - 1206

International Journal of ELECTROCHEMICAL SCIENCE
www.electrochemsci.org

Use of *Artemisia Mesatlantica* Essential Oil as Green Corrosion Inhibitor for Mild Steel in 1 M Hydrochloric Acid Solution

K. Boumhara[1], *F. Bentiss*[2], *M. Tabyaoui*[1,3,*], *J. Costa*[4], *J.-M. Desjobert*[4], *A. Bellaouchou*[3], *A. Guenbour*[3], *B. Hammouti*[5], *S.S. Al-Deyab*[6]

[1] Laboratoire de Chimie Organique, Bioorganique et Environnement, Université Chouaib Doukkali, Faculté des Sciences, B.P. 20, M-24000 El Jadida, Morocco
[2] Laboratoire de Catalyse et de Corrosion des Matériaux (LCCM), Faculté des Sciences, Université Chouaib Doukkali, B.P. 20, M-24000 El Jadida, Morocco
[3] Laboratoire des Matériaux, Nanoparticules et Environnement, Université Mohamed V Agdal, Faculté des Sciences, 4 Av. Ibn Battouta, B.P. 1014 RP, M-10000 Rabat, Morocco
[4] Laboratoire de Chimie des Produits Naturels, Faculté des Sciences et techniques, Université de Corse, UMR CNRS 6134, Corse, France
[5] LCAE-URAC18, Faculté des Sciences, Université Mohammed Premier, B.P. 717, 60000 Oujda, Morocco
[6] Petrochemical Research Chair, Department of Chemistry, College of Science, King Saud University, B.O. 2455, Riaydh 11451, Saudi Arabia
[*]E-mail: hamidtabyaoui@yahoo.fr

Received: 26 August 2013 / *Accepted:* 27 November 2013 / *Published:* 5 January 2014

The essential oil from aerial parts (stalks, leaves and flowers) of *Artemisia Mesatlantica*, was obtained by hydrodistillation and analyzed by GC and GC/MS. The main components of *Artemisia Mesatlantica* were β-thujone (33.9%) followed by camphor (7.5%), 1,8-cineole (6.9%) and α-thujone (5.5%). *Artemisia Mesatlantica* essential oil (AMEO) was tested as corrosion inhibitor of mild steel in 1 M HCl using weight loss measurements. The obtained results showed that inhibition efficiency increases with increasing inhibitor concentration to attain 91 % at 2.76 g/L of AMEO at 303 K. Physical adsorption is proposed for the corrosion inhibition mechanism and the process followed the kinetic/thermodynamic model of El-Awady et al. in the temperature range from 303 to 343 K. The adsorption and kinetic parameters for mild steel/AMEO/1 M HCl system were calculated from experimental gravimetric data and the interpretation of the results are given.

Keywords: Artemisia Mesatlantica; Essential oil; Corrosion inhibition; Mild steel; Acid; Adsorption

1. INTRODUCTION

The genus *Artemisia* (Asteraceae family, Anthemideae tribe) comprises more than 300 species

and is widespread in temperate areas such as South Europe, North Africa, North America, and Asia [1]. *Artemisia* herba-alba is a particular species in North Africa (found in Morocco to Egypt). In Morocco essential oil of the aerial part of *Artemisia herba-alba* has been studied and large chemical variability has been reported [2]. The study made on about 80 populations by Ben Jilali [3], identified in the essential oil about eight different chemotypes corresponding to well known regions of Morocco. *Artemisia Mesatlantica* Maire is one of these chemotypes. It was classified by the UICN (Union International de Conservation de la Nature en Afrique du Nord) [4] as an endemic species of Morocco, rare and in danger (Inventaire de la biodiversité, 2005) [5]. The species is very widespread between Boulmane and Ifrane in the Middle Atlas of Morocco [6]. Its blue essential oil is much studied. It reveals in its composition the presence of the following compounds: β-thujone (61%), α-thujone (3.8), borneol (1.4%), some camphor, cineol-1,8 and the fenchol [7].

Steel, an alloy of iron is widely used in petrochemical, chemical and metallurgical industries. It is also used as a construction material owing to its excellent mechanical properties and cost effectiveness. However, it easily undergoes corrosion in various environmental conditions especially in acid medium. Most well known acid inhibitors are organic compounds containing nitrogen, sulphur, and oxygen atoms. It is generally accepted that organic molecules inhibit corrosion by adsorption on metal surface [8-14]. Furthermore, the adsorption depends on the electronic structure of inhibiting molecules, steric factor, aromaticity and electron density at donor site, presence of functional group such as –C=O, -N=N-, R-OH, etc., molecular area, molecular weight of the molecule, temperature and electrochemical potential at the metal/solution interface [15-19]. Temperature dependence of the inhibitor efficiency and the comparison of the obtained thermodynamic data of the corrosion process both in absence and presence of inhibitors lead to some conclusions concerning the mechanism of inhibiting action [20-25]. Green corrosion inhibitors are biodegradable and do not contain heavy metals or other toxic compounds. The successful uses of naturally occurring substances to inhibit the corrosion of metals in acidic and alkaline environment have been reported by several workers [26-35]. In the present work, the chemical composition of *Artemisia Mesatlantica* essential oil (AMEO) is established using GC and GC-MS. Then, the inhibition performance of AMEO was evaluated by weight loss measurement at different temperatures (298–333 K) and the thermodynamic parameters for both adsorption and activation processes were calculated and discussed.

2. EXPERIMENTAL

2.1. Plant material

The aerial parts (stalks, leaves and flowers) of *Artemisia Mesatlantica* were harvested in March 2008 (full bloom) from Ifrane, Morocco. Voucher specimens were deposited in the herbarium of the Institute of Agronomic and Veterinary (IAV) Hassan II, Rabat, Morocco.

2.1.1. Essential oil isolation

Fresh vegetal material (stalks, leaves and flowers) was water distillated (4 h) using a

Clevenger-type apparatus according to the method recommended in the European Pharmacopoeia [36]. The essential oil yields were 0.7% (w/w) according to the dry material. The oils were dried over anhydrous sodium sulfate and then stored in sealed glass vials at 4–5 °C in the darkness prior to analysis.

2.1.2. Gas chromatography analysis (GC-FID)

GC analysis was carried out using a Perkin-Elmer Autosystem XL GC apparatus (Waltham, MA, USA) equipped with a dual flame ionization detection (FID) system and the fused-silica capillary columns (60 m × 0.22 mm I.D., film thickness 0.25 μm) Rtx-1 (polydimethylsiloxane) and Rtx-wax (polyethyleneglycol). The oven temperature was programmed from 60 °C to 230 °C at 2 °C/min and then held isothermally at 230 °C for 35 min. Injector and detector temperatures were maintained at 280 °C. Samples were injected in the split mode (1/50) using helium as a carrier gas (1 mL/min) and a 0.2 μL injection volume of pure oil. Retention indices (RI) of compounds were determined relative to the retention times of a series of *n*-alkanes (C_5–C_{30}) (Restek, Lisses, France) with linear interpolation using the Van den Dool and Kratz equation [37] and software from Perkin-Elmer.

2.1.3. Gas chromatography mass spectrometry (GC-MS)

Samples were analyzed with a Perkin-Elmer turbo mass detector (quadrupole) coupled to a Perkin-Elmer Autosystem XL equipped with the fused-silica capillary columns Rtx-1 and Rtx-wax. Carrier gas: helium (1 mL/min), ion source temperature: 150 °C, oven temperature programmed from 60 °C to 230 °C at 2 °C/min and then held isothermally at 230 °C (35 min), injector temperature: 280 °C, energy ionization: 70 eV, electron ionization mass spectra were acquired over the mass range 35–350 Da, split: 1/80, injection volume: 0.2 μL of pure oil.

2.1.4. Components identification

Identification of individual components was based i) on comparison of calculated RI, on polar and apolar columns, with those of authentic compounds or literature data [38]; National Institute of Standards and Technology [39]; and ii) on computer matching with commercial mass spectral libraries [40]; and comparison of mass spectra with those of our own library of authentic compounds or literature data [38,40].

2.2. Corrosion test

The gravimetric measurements were carried out at the definite time interval of 6 hours using an analytical balance (precision ± 0.1 mg). The mild steel specimens used have a rectangular form (length = 3 cm, width = 1 cm, thickness = 0.06 cm). The acid solutions (1 M HCl) were prepared by dilution of an analytical reagent grade 37 % HCl with doubly distilled water. Gravimetric experiments were

carried out in a 50 ml flask, which contained 30 ml of 1 M HCl in absence and presence of different concentration of *Artemisia Mesatlantica* essential oil (AMEO). The concentration range of AMEO used in the corrosion tests was 0.65 to 2.76 g/L. After six hours, the specimen was taken out, washed, dried and weighed accurately. The temperature effect was studied, and then the tests were repeated at different inhibitor concentrations for each temperature. The material used in this study is a mild steel with a chemical composition (in wt%) of 0.09 % P, 0.38 % Si, 0.01 % Al, 0.05 % Mn, 0.21 % C, 0.05 % S, and balance Fe were pre-treated prior to the experiments by grinding with emery paper SiC (grades 400, 600 and 1200), then cleaned in ultrasonic bath with ethanol, rinsed with bidistilled water and finally dried at room temperature.

3. RESULTS AND DISCUSSION

3.1. Essential oil composition

The analysis of essential oil from *Artemisia Mesatlantica* was carried out by CG/FID and CG/SM. The chemical composition of essential oil was characterized by 29 compounds, which accounted for 82.9% of the total oil. The retention time of volatile compounds (*RI*a and *RI*p) and their percentage are summarized in Table 1. The oil was dominated by oxygenated monoterpenes (62.0%) followed by monoterpenic hydrocarbons (11.0%). The sesquiterpene hydrocarbons and oxygenated sesquiterpenes accounted only for 3.7% and 6.2% of the total oil, respectively. The essential oil was characterized by high amounts of β-thujone **12** (33.9%). The other major components were camphor **14** (7.5%), 1,8-cineole **8** (6.9%) and α-thujone **11** (5.5%). The 24 other compounds are reported in low amounts in *Artemisia Mesatlantica* essential oil from Morocco. It should be noted that several studies have been published on chemical composition of *Artemisia Mesatlantica*. The study made by Holemann et al. [41] on the region between Ifrane and Boulmane, showed that the composition of the essential oil was rich in β-thujone (60%). In the same year and the same region, Ouyahya et al. [42] made a study who pointed out a rich composition on *β*-thujone (34%) and camphor (32%). Benchekroun et al. [43] give a close composition to the one we obtained; β-thujone (56.33%), camphene (7.48%), camphor (4.17%), 1,8-cineol (2.63%), α-thujone (1.38%); the difference observed in the chemical composition of *Artemisia Mesatlantica* for the same region can be explained by the techniques used for the extraction.

In general, this variation in the chemical composition can be understandable according to exogenous factors: the period of sunshine, the nature and the composition of the ground [44]. The *Artemisia Mesatlantica* essential oil composition is comparable to *A. herba-alba* only for the chrysanthenon compound [45-48]. The study made by Benabdellah et al [49] about the chemical composition of the *A. herba alba* oil from Ain Es-sefra (Algeria, 819 m of altitude) revealed that the main compounds obtained were β-thujone (31.50-41.23%), camphor (16.20-24.58%), 1,8-cineole (0.12-9.86%) and α-thujone (2.25-5.55%). This composition is close to the one we found for *Artemisia Mesatlantica* located in Ifrane with a minor difference for same compounds.

Table 1. Chemical composition of *Artemisia Mesatlantica* essential oil from Morocco.

N° [a]	Components	RI *l* [b]	RI *a* [c]	RI *p* [d]	% [e]
1	α-Thujene	932	924	1015	0.3
2	α-Pinene	936	932	1015	0.9
3	Camphene	950	945	1065	0.8
4	Sabinene	973	968	1119	6.0
5	β-Pinene	978	973	1108	0.4
6	α-Terpinene	1013	1011	1174	0.5
7	*p*-Cymene	1015	1015	1260	1.1
8	1,8-Cineole	1024	1024	1210	6.9
9	γ-terpinene	1051	1051	1238	1.0
10	(*E*)-Sabinene hydrate	1053	1055	1456	0.3
11	α-Thujone	1089	1088	1412	5.5
12	β-Thujone	1103	1104	1433	33.9
13	*transp*-Menth-2-en-1-ol	1116	1115	1552	0.4
14	Camphor	1123	1129	1504	7.5
15	*trans*-Sabinol	1120	1129	1685	1.0
16	Borneol	1150	1154	1685	1.6
17	3-Thujen-10-al	1158	1161	1599	0.2
18	Terpinen-4-ol	1164	1167	1592	3.2
19	Myrtenal	1172	1172	1621	0.1
20	α-Terpineol	1176	1177	1683	0.9
21	Myrtenol	1178	1179	1767	0.4
22	Piperitone	1226	1229	1704	0.1
23	(E)-β-Caryophyllene	1421	1417	1584	0.5
24	Germacrene D	1479	1477	1691	2.2
25	Bicyclogermacrene	1494	1490	1712	0.7
26	δ-Cadinene	1520	1515	1735	0.3
27	Caryophyllene oxide	1578	1570	1955	1.3
28	Ledol	1600	1593	2004	1.0
29	τ-Muurolol	1633	1620	2102	3.9
	Total identified				82.9
	Monoterpene hydrocarbons				11.0
	Oxygenated monoterpenes				62.0
	Sesquiterpene hydrocarbons				3.7
	Oxygenated sesquiterpenes				6.2

[a] The numbering refers to elution order on apolar column (Rtx-1)
[b] RI *l* = retention indices on the apolar column of literature (König et al., 2001; National Institute of Standards and Technology, 2008)
[c] RI *a* = retention indices on the apolar column (Rtx-1)
[d] RI *p* = retention indices on the polar column (Rtx-Wax)
[e] Relative percentages of components (%) are calculated on GC peak areas on the apolar column (Rtx-1) ; Values expressed are means of three parallel measurements

3.2. Corrosion inhibition evaluation

3.2.1. Effect of inhibitor concentration

The effect of addition of *Artemisia Mesatlantica* essential oil (AMEO) tested at different concentrations on the corrosion of mild steel in 1 M HCl solution was studied by weight loss measurements at 298 K after 6 h of immersion period. The corrosion rate (C_R) and inhibition efficiency η(%) were calculated according to the Eqs. 1 and 2 [50], respectively:

$$C_R = \frac{W_b - W_a}{At} \quad (1)$$

$$\eta(\%) = \left(1 - \frac{wi}{w_0}\right) \times 100 \quad (2)$$

where W_b and W_a are the specimen weight before and after immersion in the tested solution, w_0 and w_i are the values of corrosion weight losses of mild steel in uninhibited and inhibited solutions, respectively, A the area of the mild steel specimen (cm^2) and t is the exposure time (h).

The values of percentage inhibition efficiency η(%) and corrosion rate (C_R) obtained from weight loss method at different concentrations of AMEO at 303 K are summarized in Table 2. It is very clear that the AMEO inhibits the corrosion of mild steel in 1 M HCl solution, at all concentrations used in this study, and the corrosion rate (C_R) decreases continuously with increasing essential oil concentration at 303 K. Indeed, corrosion rate values of mild steel decrease when the inhibitor concentration increases while η(%) values of AMEO increase with the increase of the concentration, the maximum η(%) of 91 % is achieved at 2.76 g/L.

Table 2. Corrosion parameters obtained from weight loss measurements for mild steel in 1 M HCl containing various concentrations of AMEO at 303 K.

Inhibitor	**C_{inh} (g/L)**	**C_R ($mg.cm^{-2}.h^{-1}$)**	**η (%)**
Blank	—	2.111	**—**
AMEO	0.65	0.275	**87.0**
	1.20	0.246	**88.3**
	1.57	0.220	**89.6**
	1.84	0.211	**90.0**
	2.76	**0.189**	**91.0**

3.2.2. Effect of temperature

The effect of temperature on the inhibited acid–metal reaction is very complex, because many changes occur on the metal surface such as rapid etching, desorption of inhibitor and the inhibitor itself may undergo decomposition [51]. However, it was found that few inhibitors with acid-metal systems

have specific reactions which are effective at high temperature as (or more) they are at low temperature [52,53].

Table 3. Corrosion parameters obtained from weight loss for mild steel in 1 M HCl containing various concentrations of AMEO at different temperatures.

Temperature (K)	C_{inh} (g/L)	C_R (mg.cm^{-2}.h^{-1})	η (%)	□
303	Blank	2.111	—	—
	0.65	0.275	87.0	0.870
	1.20	0.246	88.3	0.883
	1.57	0.220	89.6	0.896
	1.84	0.211	90.0	0.900
	2.76	0.189	91.0	0.910
313	Blank	3.864	—	—
	0.65	0.978	74.7	0.747
	1.20	0.859	77.8	0.778
	1.57	0.794	79.5	0.795
	1.84	0.731	81.1	0.811
	2.76	0.558	85.6	0.856
323	Blank	8.100	—	—
	0.65	2.349	71	0.710
	1.20	2.017	75.1	0.751
	1.57	1.719	78.8	0.788
	1.84	1.583	80.4	0.804
	2.76	1.414	82.5	0.825
333	Blank	10.497	—	—
	0.65	4.308	58.9	0.589
	1.20	4.145	60.5	0.605
	1.57	3.900	62.8	0.628
	1.84	3.519	66.5	0.665
	2.76	3.242	69.1	0.691
343	Blank	19.642	—	—
	0.65	12.81	34.8	0.348
	1.20	11.08	43.6	0.436
	1.57	10.69	45.6	0.456
	1.84	9.87	49.7	0.497
	2.76	9.25	52.9	0.529

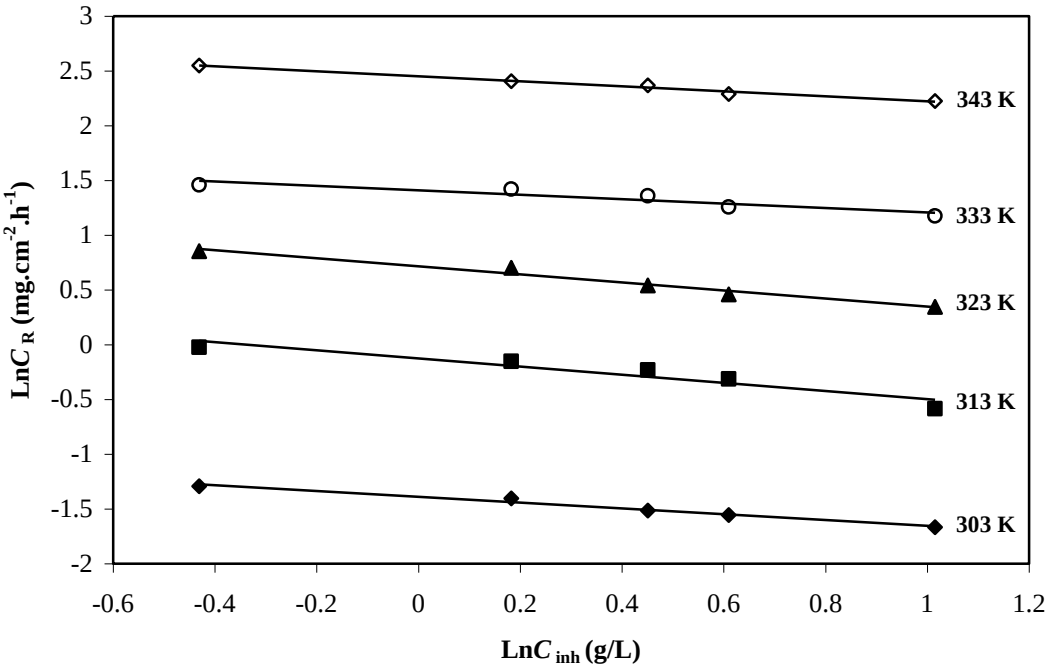

Figure 1. Variation of LnC_R with LnC_{inh} for mild steel in 1 M HCl containing AMEO.

The change of the corrosion rate at selected concentrations of the AMEO during 6 h of immersion with the temperature was studied in 1 M HCl, both in absence and presence of essential oil. For this purpose, gravimetric experiments were performed at different temperatures (303–343 K). It is clear from Table 3 that the increase in corrosion rate (C_R) is more pronounced with increasing temperature for blank solution. In the presence of the AMEO molecules, the corrosion rate of mild steel decreases at any given temperature as inhibitor concentration increases due to the increase of the degree of surface coverage. In contrast, at constant inhibitor concentration, the corrosion rate increases as temperature rises.

Assuming that the corrosion rate of mild steel against the concentration of the studied inhibitor obeys the following kinetic relationship [54,55]:

$$\mathrm{Ln}C_R = B\mathrm{Ln}C_{inh} + \mathrm{Ln}k \quad (3)$$

where k is the rate constant and equal to C_R at inhibitor concentration of unity, B is the reaction constant which in the present case is a measure of the inhibitor effectiveness and C_{inh} is the inhibitor concentration. Fig. 1 represents the curves of LnC_R versus LnC_{inh} at different studied temperatures. The straight lines show that the kinetic parameters (k and B) could be calculated by Eq. 3, and listed in Table 4.

The negative sign for the values of B indicates that the rate of corrosion process is inversely proportional to the inhibitor concentration, meaning that the inhibitor becomes more effective with increasing its concentration. So, when the change of C_R with inhibitor concentration becomes steep (high negative value for constant B) it reflects good inhibitive properties for the studied inhibitor. Moreover, the k value increases with rising temperature and its magnitude at each temperature is

comparable to that recorded in Table 1 for the analogous system containing 1.2 g/L of AMEO which indicates the validity of Eq. (3). We can note also from Table 3 that the inhibition efficiency depends on the temperature and decreases with the rise of temperature from 303 to 343 K. This can be explained by the decrease in the strength of the adsorption process at elevated temperature and suggest a physical adsorption mode [56].

Table 4. Kinetic parameters for the corrosion of mild steel in 1 M HCl containing AMEO at different temperatures.

Temperature (K)	*B*	*k* (mg.cm^{-2}.h^{-1})
303	-0.265	0.249
313	-0.371	0.883
323	-0.367	2.043
333	-0.204	3.515
343	-0.228	11.602

3.2.3. Adsorption isotherm and thermodynamic parameters

Adsorption isotherms are usually used to describe the adsorption process. The most frequently used isotherms include: Langmuir, Frumkin, Hill de Boer, Parsons, Temkin, Flory–Huggins, Dhar–Flory–Huggins, Bockris–Swinkels and the recently formulated thermodynamic/kinetic model of El-Awady et al. [57-59]. The establishment of adsorption isotherms that describe the adsorption of a corrosion inhibitor can provide important clues to the nature of the metal–inhibitor interaction. Adsorption of the organic molecules occurs as the interaction energy between molecule and metal surface is higher than that between the H_2O molecule and the metal surface [60]. The best correlation between the experimental results and isotherm functions was obtained using the Langmuir adsorption isotherm interpreted by the following equation [61]:

$$\frac{C_{inh}}{\theta} = \frac{1}{K_{ads}} + C_{inh} \quad (4)$$

where C_{inh} is the inhibitor bulk concentration in g/L, K_{ads} in g/L is the equilibrium constant of adsorption. The fractional surface coverage θ can be easily determined from weight loss measurements by the ratio η(%) / 100, if one assumes that the values of η(%) do no differ substantially from surface coverage (Table 3). Though the plot of C_{inh}/θ vs. C_{inh} was linear (Fig. 2) (correlation > 0.99), the deviation of the slopes from unity, especially at high temperature (Table 5), can be attributed to the molecular interaction among the adsorbed inhibitor species, a factor which was not taken into consideration during the derivation of the Langmuir equation. Langmuir isotherm assumes that:

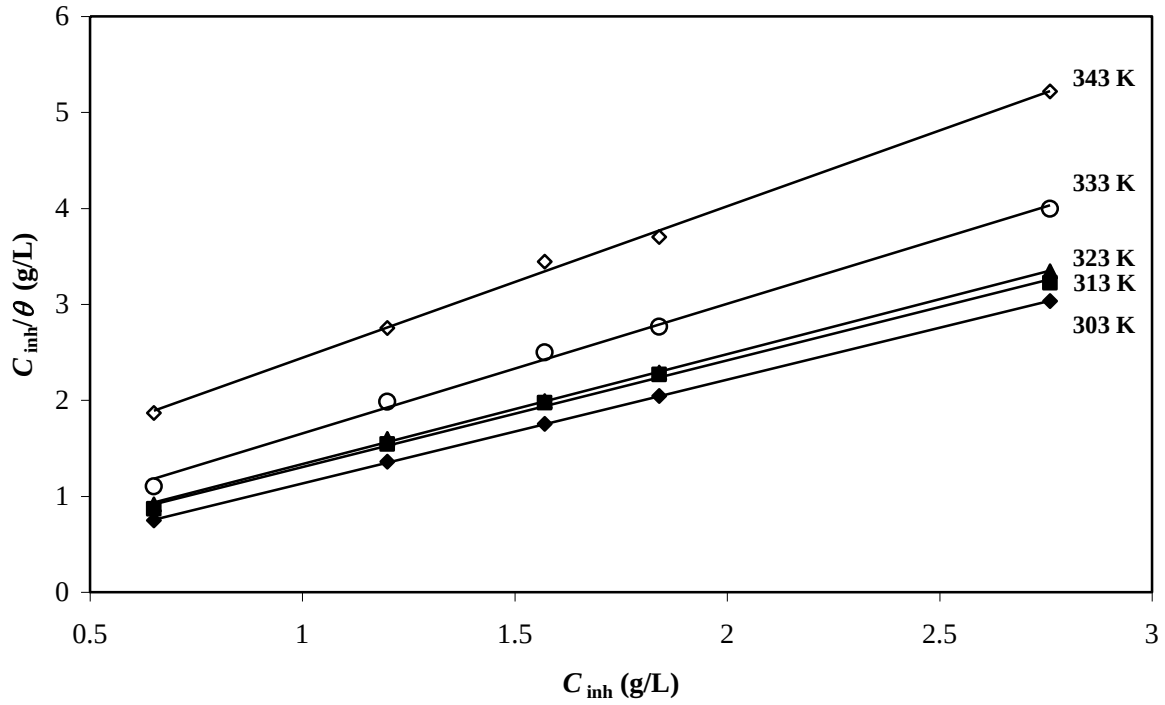

Figure 2. Langmuir's isotherm adsorption model of AMEO on the mild steel surface in 1 M HCl at different temperatures.

Table 5. Adsorption parameters for AMEO in 1 M HCl obtained from Langmuir adsorption isotherm at different temperatures.

Temperature (K)	R^2	Slope
303	0.9999	**1.08**
313	0.9981	**1.11**
323	0.9995	**1.14**
333	0.9962	**1.35**
343	**0.9976**	**1.58**

(*i*) The metal surface contains a fixed number of adsorption sites and each site holds one adsorbate.

(*ii*) ΔG^{o}_{ads} is the same for all sites and it is independent of θ.

(*iii*) The adsorbates do not interact with one another, i.e. there is no effect of lateral interaction of the adsorbates on ΔG^{o}_{ads} [62].

Though the linearity of the Langmuir plots (Fig. 2) may be interpreted to suggest that the experimental data for AMEO obey the Langmuir adsorption isotherm. However, the deviation of the slope from unity showed that the isotherm cannot be strictly applied. Hence, the experimental data were fitted into the El-Awady's kinetic/thermodynamic model. The characteristic of the isotherm is given by [63]:

$$\mathrm{Ln}\frac{\theta}{1-\theta} = \mathrm{Ln}K + y\mathrm{Ln}C_{\mathrm{inh}} \quad (5)$$

where C_{inh} is the molar concentration of inhibitor, □ is the degree of surface coverage, K is a constant related to the equilibrium constant of the adsorption process, K_{ads}, by the following relationship:

$$K_{\mathrm{ads}} = K^{\frac{1}{y}} \quad (6)$$

where y is the number of inhibitor molecules occupying one active site and 1/y represents the number of active sites of the metal surface occupied by one molecule of inhibitor. Curve fitting of the data to the thermodynamic–kinetic model is shown in Fig. 3. This plot gave straight lines which clearly showed that the data fitted well to the isotherm. The values of 1/y and K_{ads} calculated from the El-Awady et al. model curve is given in Table 6. All values of 1/y are greater than one, suggesting that a given inhibitor molecule occupies more than one active site [64]. The decreasing value of K_{ads} with increase in temperature indicates that adsorption of AMEO on the mild steel surface was unfavourable at higher temperatures. K_{ads} is related to the standard Gibbs energy of adsorption, $\Delta G^{\mathrm{o}}_{\mathrm{ads}}$, according to [65]:

$$K_{\mathrm{ads}} = \frac{1}{C_{\mathrm{H_2O}}}\exp\left(\frac{-\Delta G^{\mathrm{o}}_{\mathrm{ads}}}{RT}\right) \quad (7)$$

where R is the universal gas constant, T the thermodynamic temperature and the concentration of water in the solution is 1000 g/l. The calculated $\Delta G^{\mathrm{o}}_{\mathrm{ads}}$ values, using Eq. 7, were given in Table 6.

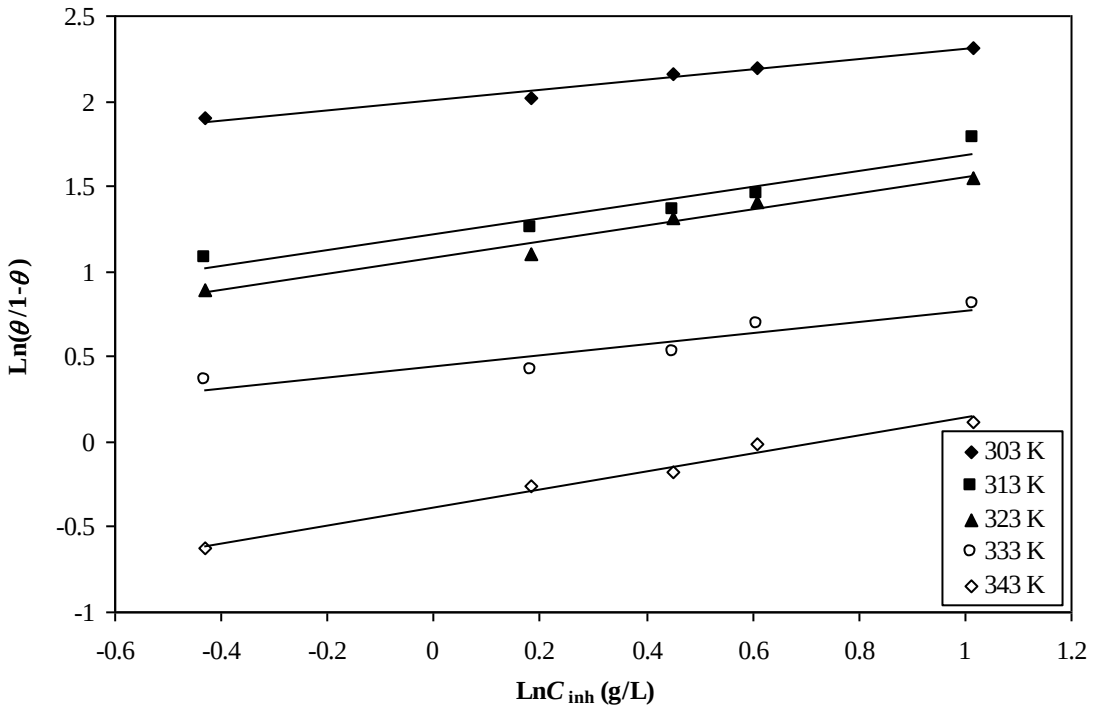

Figure 3. El-Awady's isotherm adsorption model of AMOE on the mild steel surface in 1 M HCl at different temperatures.

Table 6. Calculated parameters for El-Awady adsorption isotherm in the presence of AMEO in 1 M HCl at different temperatures.

Temperature (K)	***K*** **(g/L)**	$\frac{1}{y}$	K_{ads} **(g/L)**	ΔG^{o}_{ads} **(kJ.mol^{-1})**	R^2
303	7.46	3.4	927.5	-34.61	**0.98**
313	3.37	2.15	13.63	-24.77	**0.92**
323	2.95	2.11	9.80	-24.68	**0.97**
333	1.56	3.12	4.00	-22.96	**0.98**
343	**0.68**	**1.91**	**0.48**	**-17.61**	**0.98**

Generally, the energy values of $\Delta G°_{ads}$ around –20 kJ mol^{-1} or less negative are associated with an electrostatic interaction between charged inhibitor molecules and charged metal surface, physisorption; those of –40 kJ mol^{-1} or more negative involve charge sharing or transfer from the inhibitor molecules to the metal surface to form a coordinate type bond i.e. chemisorptions [66,67]. It is difficult to distinguish between chemisorption and physisorption only based on these criteria, especially when charged species are adsorbed. The possibility of Coulomb interactions between adsorbed cations and specifically adsorbed anions can increase the Gibb's energy even if no chemical bond appears. Here, the calculated ΔG^{o}_{ads} values are ranging between –34.61 and –17.61 kJ mol^{-1}, indicating that the adsorption mechanism of AMEO on mild steel in 1 M HCl solution at the studied temperatures is mainly du to the physisorption (ionic). The obtained values of ΔG^{o}_{ads} show the regular dependence of ΔG^{o}_{ads} on temperature (Table 6), indicating a good correlation among thermodynamic parameters and that the physisorption has the major contribution in the AMEO inhibition mechanism [68].

Assuming thermodynamic model, corrosion inhibition of mild steel in the presence of AMEO can be better explained, therefore, the standard enthalpy (ΔH^{o}_{ads}) and entropy (ΔS^{o}_{ads}) of the adsorption process were calculated. The thermodynamic parameters ΔH^{o}_{ads} and ΔS^{o}_{ads} can be calculated from the following equation (Method 1):

$$\Delta G^{o}_{ads} = \Delta H^{o}_{ads} - T\ \Delta S^{o}_{ads} \quad (8)$$

A plot of ΔG^{o}_{ads} vs. T gives straight lines (Fig. 4) with the slope equal to $-\Delta S^{o}_{ads}$, and the value of ΔH^{o}_{ads} can be calculated from intercept (Table 7).

It has been found that the ΔH^{o}_{ads} value is negative, suggesting that the adsorption of *Artemisia Mesatlantica* essential oil (AMEO) is an exothermic process. The negative value of ΔH^{o}_{ads} also indicated that the inhibition efficiency decreased with increase in temperature (Table 2) [69]. The large decrease in inhibition efficiency, from 91 to 52.9%, at 2.76g/L for example, with rise in temperature from 303 to 343 K can be attributed to its larger value of ΔH^{o}_{ads} (−142.2 kJ mol^{-1}).

Table 7. Thermodynamic parameters for the adsorption of AMEO on mild steel in 1 M HCl at different temperatures.

Temperature (K)	ΔH^{o}_{ads} **(kJ.mol^{-1})**	ΔS^{o}_{ads} **(J.mol^{-1}K^{-1})**	ΔH^{o}_{ads} **(kJ.mol^{-1})**	ΔS^{o}_{ads} **(J.mol^{-1}K^{-1})**	ΔH^{o}_{ads} **(kJ.mol^{-1})**	ΔS^{o}_{ads} **(J.mol^{-1}K^{-1})**
	Method 1		*Method 2*		*Method 3*	
303		-358.1		-363.28		-355.08
313	-140.59		-142.27		-142.2	-375.17
323						-363.84
333						-358.08
343						-363.36

Such behaviour can be interpreted on the basis that at higher temperature more desorption of the adsorbed inhibitor molecules occurred from the mild steel surface. The negative value of ΔS^{o}_{ads} is generally explained an ordered of adsorbed molecules of inhibitor with the progress in the adsorption onto the steel surface [70]. ΔH^{o}_{ads} and ΔS^{o}_{ads} values can be also calculated according to the Van't Hoff equation (Method 2) [71]:

$$\ln K_{ads} = -\frac{\Delta H^{o}_{ads}}{RT} + \text{constant} \quad (9)$$

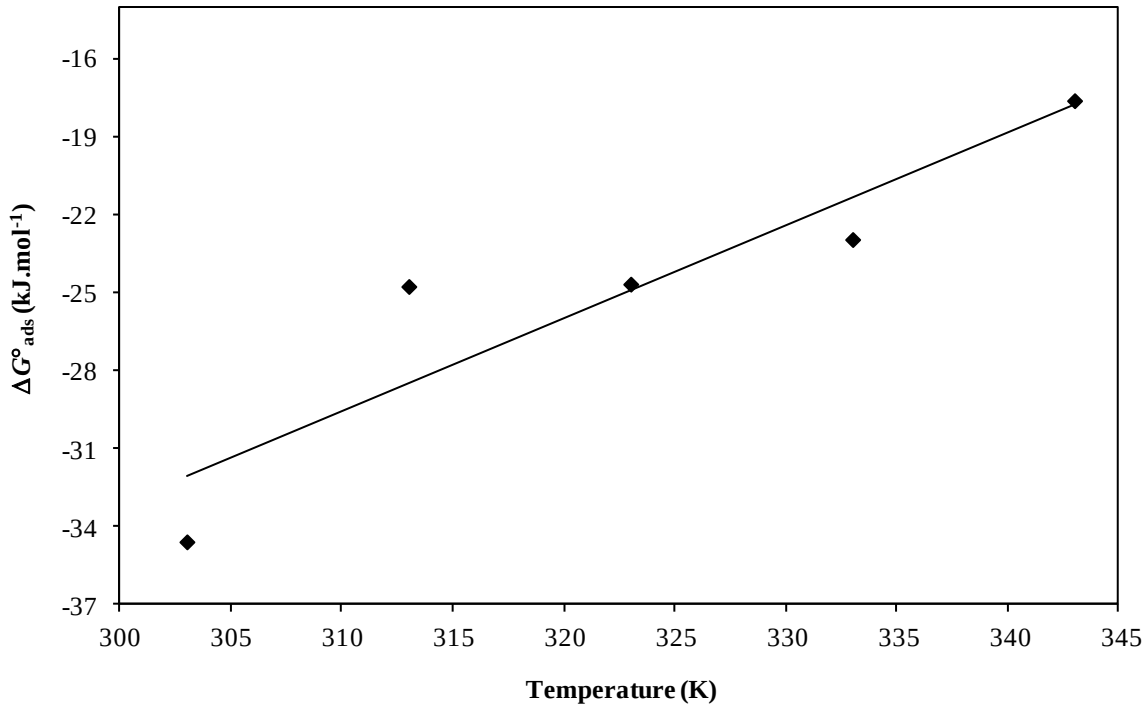

Figure 4. Variation of ΔG^{o}_{ads} versus T on mild steel in 1 M HCl containing AMEO.

A plot of Ln K_{ads} versus 1/T gives a straight line, as shown in Figure 5. The slope of the straight line is $-\Delta H^{o}_{ads}/R$ and the intercept is ($\Delta S^{o}_{ads}/R$ + ln1/C_{H20}). The obtained values of ΔH^{o}_{ads} and ΔS^{o}_{ads} are given in Table 7.

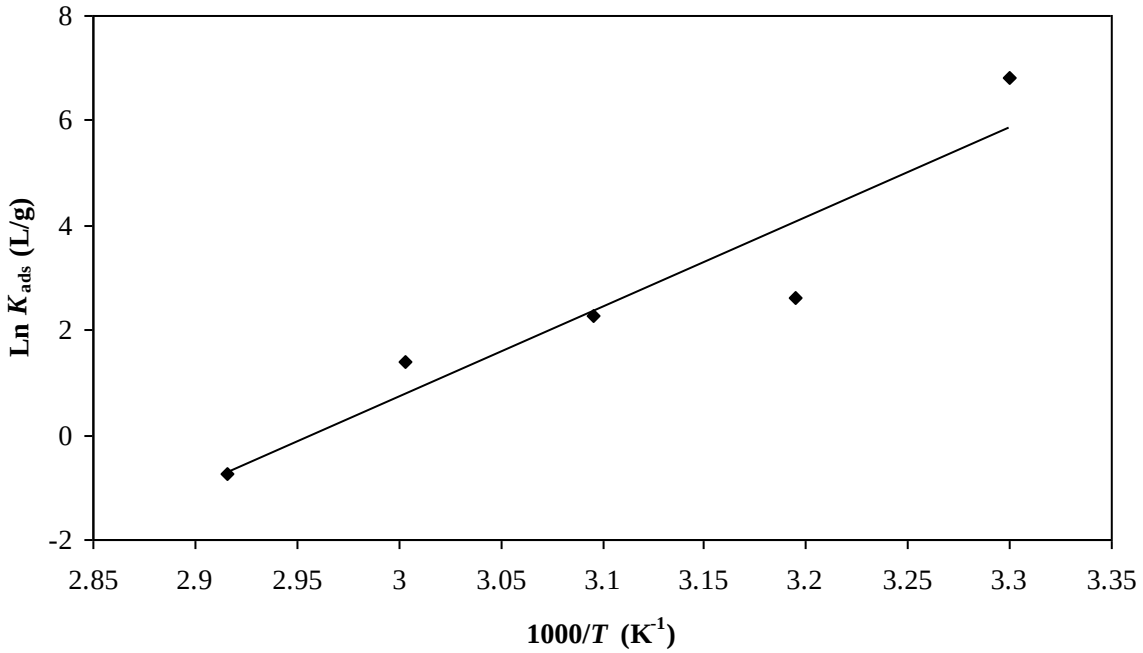

Figure 5. Vant't Hoff plot for the mild steel/AMEO/1 M HCl system.

The thermodynamic parameters (ΔH^{o}_{ads} and ΔS^{o}_{ads}) can also evaluated using the Gibbs-Helmholtz equation (Method 3), witch is defined as follow [72]:

$$\left[\frac{\partial(\Delta G^{0}_{ads}/T)}{\partial T}\right]_{p} = -\frac{\Delta H^{0}_{ads}}{T^{2}} \quad (10)$$

Eq. (10) can be arranged to give the following equation:

$$\frac{\Delta G^{0}_{ads}}{T} = -\frac{\Delta H^{o}_{ads}}{T} + \text{constant} \quad (11)$$

The variation of $\Delta G^{o}_{ads}/T$ with 1/T gives a straight line with a slope which is equal to $-\Delta H^{o}_{ads}$ (Fig. 6). It can be seen from this figure that $\Delta G^{o}_{ads}/T$ decreases with 1/T in a linear fashion. The obtained value of ΔH^{o}_{ads} was −142.2 kJ mol^{-1}. In this case, the standard adsorption entropy (ΔS^{o}_{ads}) values, given in Table 7, was calculated for all studied systems by applying the equation 8. The values of ΔH^{o}_{ads} and ΔS^{o}_{ads} obtained by the three methods are in good agreement (Table 7).

The probable mechanism of steel inhibition corrosion by AMEO can be explained on the basis of adsorption process and the structure of the constituents present in the essential oil. The adsorption may be due to the structures of the molecules present in the essential oil through the oxygen atoms on to the surface of the metal. Probably the adsorption of AMEO is made by (α/β)-thujone which is the main component of this oil.

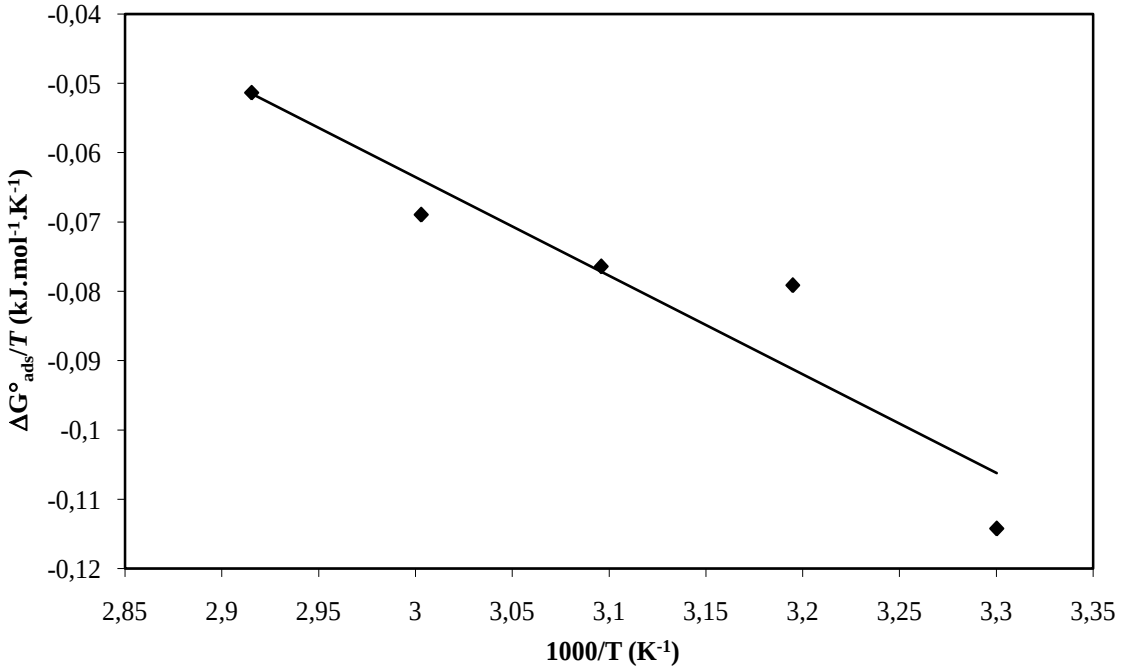

Figure 6. Relationship between $\Delta G^{o}_{ads}/T$ and the reverse of absolute temperature.

The natural oil contains so many other molecules which are able to be adsorbed on the surface steel, like the aromatic components. The inhibitory action is may be due to synergistic intermolecular of the active molecules of this oil.

3.2.4. Kinetic-thermodynamic corrosion parameters

The adsorption phenomenon has been successfully explained by thermodynamic parameter, to further elucidate the inhibition properties of inhibitor, the kinetic model was another useful tool to explain the mechanism of corrosion inhibition for the inhibitor. The activation parameters for the corrosion process of mild steel in the absence and presence of different concentrations of AMEO were calculated from Arrhenius Eq. (12) and transition state Eq. (13) in the temperature range from 303 to 343 K [50]:

$$C_R = A\exp\left(-\frac{E_a}{RT}\right) \quad (12)$$

$$C_R = \frac{RT}{Nh}\exp\left(\frac{\Delta S_a}{R}\right)\exp\left(-\frac{\Delta H_a}{RT}\right) \quad (13)$$

where E_a is the apparent activation corrosion energy, R is the universal gas constant, A is the Arrhenius pre-exponential factor, h is Plank's constant, N is Avogrado's number, ΔS_a is the entropy of activation and ΔH_a is the enthalpy of activation.

Arrhenius plots for the corrosion rate of mild steel are given in Fig. 7. Values of E_a for mild steel in 1 M HCl without and with different concentrations of AMEO were calculated by linear regression between LnC_R and 1/T. Results are shown in Table 8. All the linear regression coefficients

are close to 1, indicating that corrosion of mild steel in 1 M HCl can be elucidated using the kinetic model. The calculated value of E_a in the uninhibited solution (47.26 kJ mol^{-1}) is in the same order of magnitude as that previously described [51,64,73].

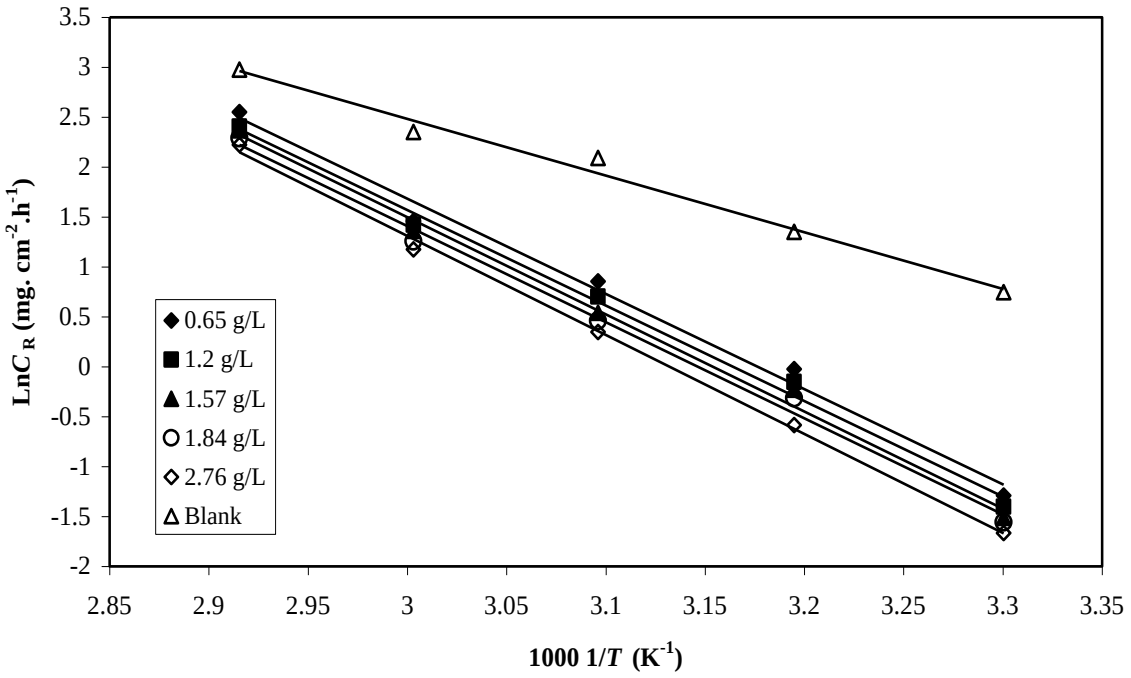

Figure 7. Arrhenius plots for mild steel corrosion rates (C_R) in 1 M HCl in absence and in presence of different concentrations of AMEO.

Table 8. Kinetic-thermodynamic corrosion parameters for mild steel in 1 M HCl in absence and presence of different concentrations of AMEO.

C_{inh} (g/L)	E_a (kJ.mol^{-1})	ΔH_a (kJ.mol^{-1})	ΔS_a (J.mol^{-1}.K^{-1})
Blank	47.26	44.59	**-91.44**
0.65	79.31	76.63	**-1.96**
1.20	79.52	76.85	**-2.25**
1.57	80.94	78.26	**-1.90**
1.84	80.08	77.41	**1.41**
2.76	**82.42**	**79.75**	**4.04**

It can be seen from the Table 8 that the E_a increased with increasing concentration of AMEO, but all values of E_a in the range of the studied concentration were higher than that obtained in the case of uninhibited solution (blank). This behaviour can suggest that higher energy barrier for the corrosion process in the inhibited solutions associated with physical adsorption or weak chemical boding between the inhibitor species and the steel surface [74,75]. Szauer et al. explained that the increase in activation energy can be attributed to an appreciable decrease in the adsorption of the inhibitor on the

steel surface with increase in temperature [76] and therefore more desorption of inhibitor molecules occurs because these two opposite processes are in equilibrium. A corresponding increase in the corrosion rate occurs because of the greater area of metal that is consequently exposed to the acid environment [77]. The kinetic-thermodynamic corrosion study is in good agreement with the finding of adsorption isotherm investigations.

The relationship between Ln (C_R/T) and $1/T$ is shown in Fig. 8. Straight lines are obtained with a slope of ($-\Delta H_a/R$) and an intercept of (Ln $R/Nh + \Delta S_a/R$) from which the values of ΔH_a and ΔS_a are calculated and presented in Table 8. Inspection of these data reveals that the ΔH_a values for dissolution reaction of mild steel are higher in the presence of AMEO (76.63 – 79.75 kJ.mol^{-1}) than that in its absence (44.59 kJ.mol^{-1}).

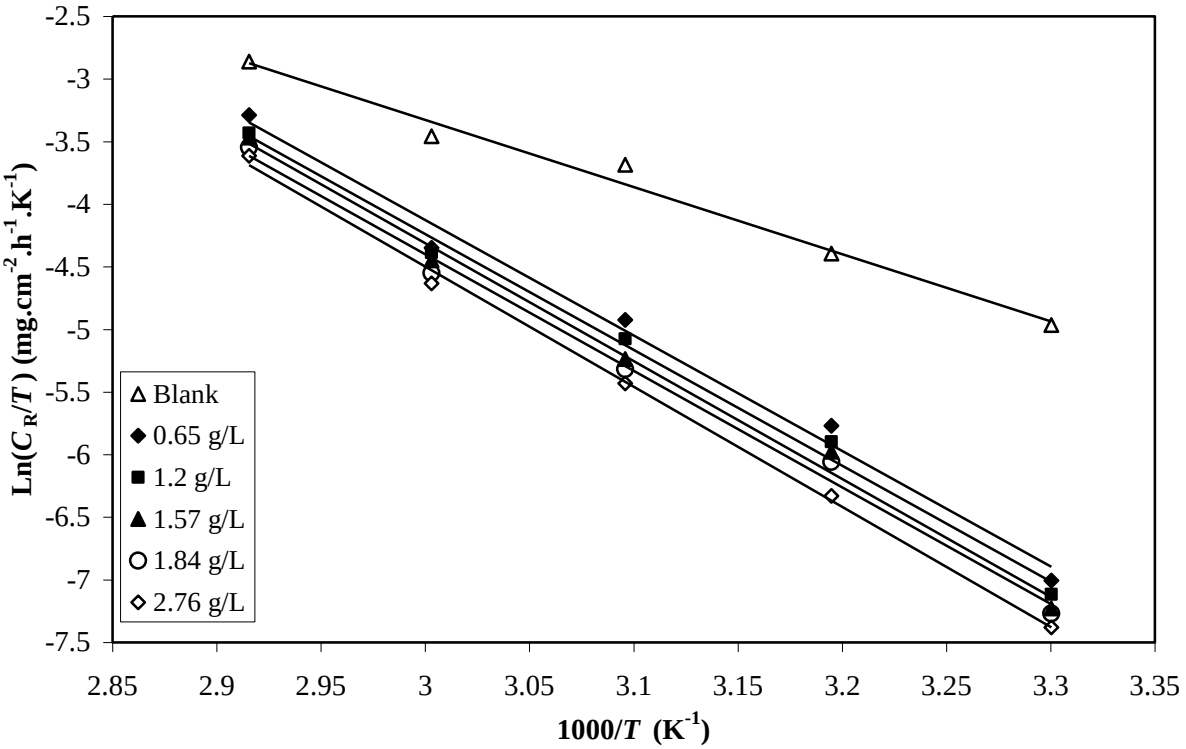

Figure 8. Transition-state plots for mild steel corrosion rates (C_R) in 1 M HCl in absence and in presence of different concentrations of AMEO.

The positive sign of ΔH_a values reflects the endothermic nature of the mild steel dissolution process. All values of E_a are larger than the analogous values of ΔH_a indicating that the corrosion process must involved a gaseous reaction, simply the hydrogen evolution reaction, associated with a decrease in the total reaction volume [56]. Moreover, for all systems, the average value of the difference E_a - ΔH_a is about 2.67 kJ.mol^{-1} which approximately around the average value of RT (2.68 kJ.mol^{-1}); where T are in the range of the experimental temperatures, indicating that the corrosion process is a unimolecular reaction as it is characterized by the following equation [78]. On comparing the values of the entropy of activation (ΔS_a) in Table 8, it is clear that ΔS_a is more positive in presence of the studied inhibitor (AMEO) compared to free acid solution. Such variation is associated with the phenomenon of ordering and disordering of inhibitor molecules on the mild steel surface. The increased entropy of activation in the presence of inhibitor indicated that disorderness is increased on

going from reactant to activated complex. This observation is in agreement with the findings of other workers [68,79-81]. This behaviour can also be explained as a result of the replacement process of water molecules during adsorption of molecule inhibitor on the steel surface and therefore the increasing in entropy of activation was attributed to the increasing in solvent entropy [82].

4. CONCLUSION

The analysis of essential oil isolated from *Artemisia Mesatlantica* plant shows that its composition is dominated by α-/β-thujone (5.5% / 33.9%, respectively). *Artemisia Mesatlantica* essential oil (AMEO) shows excellent inhibition properties for the corrosion of mild steel in 1 M HCl at 303 K, and the inhibition efficiency, η(%), increases with increase of the AMEO concentration. At 2.76 g/L M, the inhibition efficiency η(%) of AMEO is as high as 91 %. The inhibition efficiency of AMEO is found to decrease proportionally with increasing temperature (303 to 343 K) and its addition to 1 M HCl leads to increase of apparent activation energy (E_a) of corrosion process. The corrosion process is inhibited by the adsorption of AMEO on steel surface and the adsorption of the inhibitor fits a El-Awady's kinetic/thermodynamic model under all of the studied temperatures. Thermodynamic adsorption parameters show that AMEO is adsorbed on mild steel surface by an exothermic process. Moreover, the calculated values of ΔG_{ads}^{o} and ΔH_{ads}^{o} reveal that the adsorption mechanism of AMEO on steel surface in 1 M HCl solution is mainly electrostatic-adsorption.

References

1. J.A. Marco, O. Barbera. Natural products from the Genus Artemisia L. In: Atta-ur-Rahman, (Stud Nat Prod Chem. 7: 201, 1990).
2. A. Ouyahya, R. Negre, J. Viano, Y. Lozano, E.M. Gaydou, *Lebensmittlel-wisseschaft & Technologie* 23 (1990) 528.
3. B. Benjilali, J. Sarris, H. Richard, *Sci. Aliment.* 2 (1982) 515.
4. B. Benjilali, H. Richard, P. Liddle, In: Artemisi, Ricerca, Applicazione, Suppl. 2, Quaderno Agricolo (Saint Vincent, Italy, 1984).
5. B. Benjilali, H. Richard, *Riv. Ital. E.P.P.O.S.* 12 (1980) 2.
6. A. Ouyahya, *Bull. Institut Scientifique, Rabat,* 6 (1982) 89.
7. J. Bellakhder, La Pharmacopée marocaine traditionnelle. Médecine arabe ancienne et savoirs populaires. (Ibis Press, Paris France 181 1997).
8. E. Garcia-Ochoaa,, J. Genescab, *Surf. Coat. Tech*. 184 (2004) 322.
9. Y. Harek, L. Larabi, *Kem. Ind.* 2 (2004) 55.
10. N. Tantawy, the Annals of University "DUNĂREA DE JOS" of Galati Fascicle VIII, 2005, ISSN 1221-4590.
11. H. Amar, J. Benzakour, A. Derja, D. Villemin, B. Moreau, T. Braisaz, *Appl. Surf. Sci*. 252 (2006) 6162.
12. L.F. Guo, D.M. Zhang, J. Q. Meng, *Acta. Phys.Chim. Sin*. 24 (2008) 138.
13. A. Chetouani, M. Daoudi, B. Hammouti, T. Ben Hadda, M. Benkaddour, *Corros. Sci*. 48 (2006) 2987;
14. B. Mernari, H. El Attari, M. Traisnel, F. Bentiss, M. Lagrenée, *Corros. Sci*. 40 (1998) 391.

15. F. Bentiss, M. Lagrenée, M. Traisnel, B. Mernari, H. El Attari, *J. Appl. Electrochem*. 29 (1999) 1073.
16. A.K. Singh, M.A. Quraishi, *J. Appl. Electrochem.* 41 (2011) 7.
17. H.A. Abo Dief, E.A. Eissa, S.T. Keera, A.R. Taman, *J. Appl. Sci. Res.* 6 (2010) 1325.
18. F. Bentiss, C. Jama, B. Mernari, H. El Attari, L. El Kadi, M. Lebrini, M. Traisnel, M. Lagrenée, *Corros. Sci.* 51 (2009) 1628.
19. H.F. Finley, A. Hackerman, *Ind. Eng. Chem*. 46 (1960) 523;
20. U.J. Ibok, U.J. Ekpe, O.E. Ita, *Mat. Chem. Phys*. 40 (1994) 63;
21. D.K. Yadav, M.A. Quraishi, B. Maiti, *Corros. Sci.* 55 (2012) 254.
22. H.A. Abo Dief, E.A. Eissa, S.T. Keera, A.R. Taman, *J. Appl. Sci. Res*. 6 (2010) 1325.
23. M. Lebrini, M. Lagrenée, M. Traisnel, L. Gengembre, H. Vezin, F. Bentiss, *Appl. Surf. Sci*. 253 (2007) 9267.
24. S.A. Ali, A.M. El-Shareef, R.F. Al-Ghamdi, M.T. Saeed, *Corros. Sci*. 47 (2005) 2659.
25. M. Bouklah, B. Hammouti, M. Lagrenée, F. Bentiss, *Corros. Sci*. 48 (2006) 2831.
26. E. Chaieb, A. Bouyanzer, B. Hammouti, M. Benkaddour, *Appl. Surf. Sci*. 246 (2005) 199.
27. E. Chaieb, A. Bouyanzer, B. Hammouti, M. Benkaddour, M. Berrabah, *Trans. SAEST*. 39 (2004) 58.
28. L.R. Chauhan, G. Gunasekaran, *Corros. Sci*. 49 (2007) 1143.
29. A.Y. El-Etre, M. Abdallah, Z.E. El-Tantawy, *Corros. Sci*. 47 (2005) 385.
30. R. Saratha, R. Savitha, S. Sivakamasundari, *J. Electrochem. Soc. Ind*. 52 (2003) 59.
31. A.Y. El-Etre, *J. Coll. Inter. Sci*. 314 (2007) 578.
32. A. Chetouani, B. Hammouti, M. Benkaddour, *Pig. Resin. Technol*. 33 (2004) 26.
33. L.R. Chauhan, G. Gunasekaran, *Corros. Sci*. 49 (2007) 1143.
34. B.I. Ita, O.E. Effiong, *Global J. Pure Appl. Sci*. 6 (2000) 51.
35. A. Singh, E.E. Ebenso, M.A. Quraishi, *Inter. J. Corros.* Article ID 897430, 20 pages, 2012 (and references therein).
36. J.F. Clevenger, *J. Am. Pharm. Assoc*. 17 (1928) 346.
37. H. Van den Dool, P. Kratz, *J. Chromatographie* 11 (1963) 463.
38. W.A. König, D.H. Hochmuth, D. Joulain, Terpenoids and Related Constituents of Essential Oils. Library of Mass Finder 2.1 (Institute of Organic Chemistry, Hamburg, Germany, 2001).
39. National Institute of Standards and Technology. NIST WebBook (06/2005): http://webbook.nist.gov/chemistry.
40. R.P. Adams, Identification of essential oil components by Gaz chromatography/quadrupole mass spectroscopy. Allured Publishing: (Carol Stream, 2001).
41. M. Holemann, A. Idrissi, M. Berrada, *Planta Med. Apr.* 57 (1990) 198.
42. A. Ouyahya, R. Negre, J. Viano, Y. Lozano, E. M. Gaydou, *Lebensmittlel-wisseschaft & Technologie* 23 (1990) 528.
43. H.K. Benchekroun, M. Ghanmi, B. Satrani, A. Aafi, A. Chaouch, *Bull. Soc. Roy. Sc. Li*. 81 (2012) 4.
44. F.X. Garneau, corporation: LASEVE-UQAC, Chicoutimi (Quebec) G7H 2B1 Huiles essentielles: de la plante à la commercialisation – Manuel pratique « le matériel végétal et les huiles essentielles ».
45. BM. Lawrence, Progress in Essential oil, *Perfume and flavor* 6 (1981) 37 and 43.
46. BM. Lawrence, Perfumer and Flavorist (Ed.), Essential Oils 1988–1991. Allured Publishing Corporation; Carol Stream, IL: 1993. Armoise oil, Natural Flavor and Fragrance Materials; pp. 52–54.
47. B.M. Lawrence, Progress in Essential oil, *Perfume & flavor* 14 (1989) 71.
48. M. Ghanmi, B. Satrani, A. Aafi, M.R. Ismaili, H. Houti, EL Monfalouti, K.H. Benchekroun, M. Aberchane, L. Harki, A. Boukir, A. Chaouch, Z. Charrouf, *Phytothérapie* 8 (2010) 295.

49. M. Benabdellah, M. Benkaddour, B. Hammouti, M. Bendahhou, A. Aouiniti, *Appl. Surf. Sci*. 252 (2005) 6212.
50. L. Herrag, B. Hammouti, S. Elkadiri, A. Aouniti, C. Jama, H. Vezin, F. Bentiss, *Corros. Sci*. 52 (2010) 3042.
51. F. Bentiss, M. Lebrini, M. Lagrenée, *Corros. Sci*. 47 (2005) 2915.
52. B.I. Ita, O.E. Offiong, *Mater. Chem. Phys*. 70 (2001) 330.
53. M.H. Wahdan, A.A. Hermas, M.S. Morad, *Mater. Chem. Phys*. 76 (2002) 111.
54. E. Khamis, M.A. Ameer, N.M. Al-Andis, G. Al-Senani, *Corrosion* (NACE) 56 (2000) 127.
55. E.A. Noor, *Corros. Sci.* 47 (2005) 33.
56. A. El Bribri, M. Tabyaoui, B. Tabyaoui, H. El Attari, F. Bentiss, *Mater. Chem. Phys*. 141 (2013) 240.
57. E. Khamis, *Corrosion* (NACE) 46 (1990) 476.
58. S.S. Abd El-Rehim, A. Magdy, M. Ibrahim, F. Khaled, *J. Appl. Electrochem*. 29 (1999) 593.
59. E. McCafferty, in: H. Leidheiser Jr. (Ed.), Corrosion Control by Coating, Science Press, Princeton, 1979.
60. G. Moretti, G. Quartarone, A. Tassan, A. Zingales, *Mater. Corros*. 45 (1994) 641.
61. N. Labjar, M. Lebrini, F. Bentiss, N. Chihib, S. El Hajjaji, C. Jama, *Mater. Chem. Phys*. 119 (2010) 330.
62. R.F.V. Villamil, P. Corio, J.C. Rubin, S.M.I. Agostinho, *J. Electroanal. Chem*. 472 (1999) 112.
63. A. El Awady, A. Abd El Naby, S. Aziz, *J. Electrochem. Soc*. 139 (1992) 2149.
64. A.K. Singh, M.A. Quraishi, *Corros. Sci*. 53 (2011) 1288.
65. F. Bentiss, M. Lebrini, M. Lagrenée, M. Traisnel, A. Elfarouk, H. Vezin, *Electrochim. Acta* 52 (2007) 6865.
66. M.J. Bahrami, S.M.A. Hosseini, P. Pilvar, *Corros. Sci.* 52 (2010) 2793.
67. M. Behpour, S.M. Ghoreishi, N. Mohammadi, N. Soltani, M. Salavati-Niasari, *Corros. Sci*. 52 (2010) 4046.
68. E.A. Noor, A.H. Al-Moubaraki, *Corros. Sci*. 51 (2009) 868.
69. H.M. Bhajiwala, R.T. Vashi, *Bull. Electrochem*. 17 (2001) 441.
70. G. Mu, X. Li, G. Liu, *Corros. Sci*. 47 (2005) 1932.
71. M. Bouklah, B. Hammouti, M. Lagrenée, F. Bentiss, *Corros. Sci*. 48 (2006) 2831.
72. S. Bilgic, *Mater. Chem. Phys*. 76 (2002) 52.
73. F. Bentiss, M. Bouanis, B. Mernari, M. Traisnel, H. Vezin, M. Lagrenée, *Appl. Surf. Sci*. 252 (2005) 950.
74. A. Popova, E. Sokolova, S. Raicheva, M. Christov, *Corros. Sci*. 45 (2003) 33.
75. 31. X. Li, G. Mu, *Appl. Surf. Sci*. 252 (2005) 1254.
76. T. Szauer, A. Brandt, *Electrochim. Acta* 26 (1981) 1253.
77. T. Szauer, A. Brandt, *Corros. Sci* 23 (1983) 1247.
78. G.K. Gomma, M.H. Wahdan, *Mater. Chem. Phys*. 39 (1995) 209.
79. I. Ahamad, R. Prasad, M.A. Quraishi, *Corros. Sci*. 52 (2010) 933.
80. A.K. Singh, M.A. Quraishi, *Corros. Sci*. 52 (2010) 1529.
81. M. Bouklah, N. Benchat, B. Hammouti, A. Aouniti, S. Kertit, *Mater. Lett*. 60 (2006) 1901.
82. B.Ateya, B.E. El-Anadouli, F.M.El-Nizamy, *Corros. Sci*. 24 (1984) 509.